Rotation effect on geodesic and zonal flow modes in tokamak plasmas with isothermal magnetic surfaces

Plasma Phys. Control. Fusion **53** (2011) 105003 (7pp) doi:10.1088/0741-3335/53/10/105003

Rotation effect on geodesic and zonal flow modes in tokamak plasmas with isothermal magnetic surfaces

A G Elfimov, R M O Galvão and R J F Sgalla

Institute of Physics, University of São Paulo, 05508-900, São Paulo, Brazil

E-mail: elfimov@if.usp.br

Received 16 May 2011, in final form 2 August 2011
Published 25 August 2011
Online at stacks.iop.org/PPCF/53/105003

Abstract

The electrostatic geodesic mode oscillations are investigated in rotating large aspect ratio tokamak plasmas with circular isothermal magnetic surfaces. The analysis is carried out within the magnetohydrodynamic model including heat flux to compensate for the non-adiabatic pressure distribution along the magnetic surfaces in plasmas with poloidal rotation. Instead of two standard geodesic modes, three geodesic continua are found. The two higher branches of the geodesic modes have a small frequency up-shift from ordinary geodesic acoustic and sonic modes due to rotation. The lower geodesic continuum is a new zonal flow mode (geodesic Doppler mode) in plasmas with mainly poloidal rotation. Limits to standard geodesic modes are found. Bifurcation of Alfvén continuum by geodesic modes at the rational surfaces is also discussed. Due to that, the frequency of combined geodesic continuum extends from the poloidal rotation frequency to the ion-sound band that can have an important role in suppressing plasma turbulence.

1. Introduction

In the past decade, geodesic acoustic modes (GAMs) discovered in a theoretical magnetohydrodynamic (MHD) analysis [1] have attracted considerable interest due to their relevant role in the H-mode and transport barrier (TB) formation to suppress plasma turbulence. The existence of GAMs with $M = 1$, $N = 0$ poloidal/toroidal mode numbers was already experimentally confirmed [2–5]. Indeed, many theoretical and numerical investigations are currently being pursued to further understand the characteristics and effects of GAMs and the mode is the subject of active investigations in theory and simulations [6–12]. The formation of the H-mode and TB usually occurs during neutral beam (NB) or ion cyclotron resonance heating (ICRH), which are accompanied by poloidal and (or) toroidal rotation of the plasma column [3–5]. In a non-rotating plasma, the GAM frequency is $\omega^2_{\rm GAM} = \omega^2_{\rm s}(\Gamma + 1/q^2)$ where $\omega^2_{\rm s} = \gamma P/(\rho R_0^2)$, $q = rh_\zeta/h_\theta R_0$ is the safety factor, P is the plasma pressure, ρ is the

mass density, γ is the adiabatic index, R_0 is the tokamak major radius, $\Gamma = 2$ in MHD, and $\Gamma = 7/2$ in kinetic approaches [11, 12]. The oscillations are electrostatic, which depend on the parallel $(\boldsymbol{h}\cdot\boldsymbol{V})$ and binormal $(\boldsymbol{h}\times\boldsymbol{e}_r)\cdot\boldsymbol{V}$ velocities where $\boldsymbol{h} = \boldsymbol{B}/B$ is the unit vector of the magnetic field and $\boldsymbol{e}_r$ is the radial unit vector, and have poloidally symmetric radial electric field E_r. The equilibrium and oscillating field quantities are assumed to be axisymmetric and independent of the toroidal angle ζ. These oscillations do not perturb the magnetic surfaces ($\delta\boldsymbol{B} = 0$), which are assumed to be circular and concentric with the set of coordinates ($R = R_0 + r\cos\theta$, $z = r\sin\theta$, ζ) where r is the plasma surface radius. In a series of MHD [6–10] and kinetic [11] investigations, it has been shown that the toroidal flow effect on standard GAM produces a slight up-shift of the frequency $\omega^2_{\mathrm{GAM1}} \approx \omega^2_{\mathrm{s}}(2+1/q^2+4V^2/c^2_{\mathrm{s}})$. Another branch, corresponding to the zero-frequency zonal flow (ZF) in static equilibrium [7], depends directly on the toroidal rotation velocity, $\omega^2_{\mathrm{ZF}} \approx (\gamma-1)V^4/c^2_{\mathrm{s}}R^2_0$, for an isothermal equilibrium of the plasma pressure ($p_{\mathrm{eq}} \sim \rho_{\mathrm{eq}}$). The ZF may be explained as a result of an effective 'gravity' mode with the frequency [7] $\omega^2_{\mathrm{gr}} \approx V^2_\zeta(1/\gamma R)(\mathrm{d}/\mathrm{d}R)\ln(\rho^\gamma_{\mathrm{eq}}/p_{\mathrm{eq}})$. In accordance with this equation, the ZF branch becomes unstable for a constant plasma density on the magnetic surface [8]. In both approaches, it is assumed that the equilibrium is not adiabatic. We note that pure toroidal rotation [7, 8] is a degenerated case due to the possibility of using the non-adiabatic equilibrium without heat flow. For the adiabatic equilibrium with poloidal rotation in the MHD model, the ZF branch disappears [9, 10], as well as in the kinetic approach for plasmas with parallel flow [11]. In spite of different equilibria used in the last works, the results are similar, i.e. the upper mode is slightly modified by the rotation velocity but the second branch appears as an ion-sound mode modified by poloidal rotation $\omega^2_{\mathrm{GAM2}} \approx \omega^2_{\mathrm{s}}(1+3V^2_{\mathrm{pol}}/c^2_{\mathrm{s}})/q^2$. Previous investigations of the geodesic modes demonstrate that there are only two branches of the geodesic modes in rotating plasmas, which are the standard $\omega_{\mathrm{GAM1,2}}$ modes in the adiabatic approach [9, 10] and ω_{GAM1} and ω_{ZF} modes in toroidally rotating plasmas with isothermal surfaces [7, 8].

Here we are going to study the branches of the GAM continuum changing from a preferentially toroidal rotation to predominantly poloidal rotation in plasmas with isothermal magnetic surfaces using the standard MHD approach. The effect of plasma rotation on electrostatic GAM modes is investigated for large aspect ratio tokamaks ($\varepsilon = r/R_0 \ll 1$), taking into account the heat flux. Due to heat flux, we show that three geodesic modes ($\omega_{\mathrm{GAM1,2}}$ and ω_{ZF}) may appear in plasmas with toroidal and poloidal rotation.

2. Equilibrium

Generally, some poloidal rotation has to be assumed in tokamaks that may be generated due to neoclassical, ambipolar or other effects; in fact, it ubiquitously appears during the L–H mode transition [4, 5]. In this case, and considering non-adiabatic equilibria, we have to take into account the thermal flow defined by the heat balance equation [13]

$$\frac{3}{2}P\frac{\mathrm{d}}{\mathrm{d}t}(\ln\rho^\gamma - \ln P) = \nabla\boldsymbol{Q}, \qquad \boldsymbol{Q} \approx \frac{5}{2}\frac{\rho}{\omega_{\mathrm{ci}}}v^2_{\mathrm{Ti}}[\boldsymbol{h}\times\nabla v^2_{\mathrm{Ti}}] \tag{1}$$

where $\boldsymbol{Q}$ is the ion thermal flux vector where small dissipative terms are ignored. Although impurity and neoclassical effects may modify the heat flux, equation (1) is adequate to include qualitatively the basic physics in the ZF and geodesic mode analyses.

We start with the standard continuity and momentum equations, supplemented with the reduced Ohm's law as they were used in [6–10], i.e.

$$\frac{\partial\rho}{\partial t} + \nabla\cdot(\rho\boldsymbol{V}) = 0 \tag{2a}$$

$$\rho\frac{\partial \boldsymbol{V}}{\partial t}+\rho(\boldsymbol{V}\cdot\nabla)\boldsymbol{V}=-\nabla P+\frac{1}{c}\boldsymbol{J}\times\boldsymbol{B} \tag{2b}$$

$$cE_r+V_\theta B_\zeta-V_\zeta B_\theta-\frac{B}{\omega_{\rm ci}\rho}\nabla_r P=0. \tag{2c}$$

The MHD quantities are represented as a sum of time-independent equilibrium and perturbed values, $P = p_{\rm eq} + p_0\tilde{\rho}\exp(\mathrm{i}\omega t)$, $\rho = \rho_{\rm eq} + \rho_0\tilde{\rho}\exp(\mathrm{i}\omega t)$, $\boldsymbol{V} = \boldsymbol{u} + \boldsymbol{v}\cdot\exp(\mathrm{i}\omega t)$, $\boldsymbol{J} = \boldsymbol{J}_{\rm eq} + \boldsymbol{j}\cdot\exp(\mathrm{i}\omega t)$, where perturbed values are assumed to be small in comparison with the equilibrium ones. Complete equilibrium with rotation was discussed in a series of works (for example, in [6–10] and references therein) and we are going to use the simplest equilibrium, which presents the main rotation effect. We simplify the evaluation of the equilibrium using a kind of iteration process assuming subsonic rotation and $\varepsilon \ll 1$. In the first step, we define the time-independent equilibrium values considering isothermal pressure and density profiles $p_{\rm eq} \sim \rho_{\rm eq} = \rho_0(1+\varepsilon\rho_1\cos\theta)$ driven by poloidal and toroidal centrifugal and Coriolis forces, where the poloidal dependence is produced by toroidal geometry as it was used in [10]. The forces may be treated as some kind of a gravitational force with exponential density distribution that depends on the square of the rotational velocity [7–9], which is studied in the first order of ε-approximation, and we ignore the effect of second poloidal harmonic in equilibrium. The dependence of $\rho_{\rm eq}$-equilibrium on the rotation velocities will be specified from equation (2*b*) in the last step. Next, using the first-order ε-corrections in the continuity equation (2*a*), we obtain the poloidal velocity modulation $u_{\rm p} = u_0[1-\varepsilon(1+\rho_1)\cos\theta]$. Then, to satisfy the condition of constant electric field over the magnetic surfaces, we specify the toroidal rotation $u_{\rm t} = U + [\varepsilon U - u_0 q(2+\rho_1)]\cos\theta$ to equilibrate the poloidal velocity modulation. Due to this condition, we note that pure poloidal rotation is not possible. This means that preferentially poloidal rotation [9, 10] may occur only when the toroidal velocity is $u_{\rm t} = -u_0 q(2+\rho_1)\cos\theta$. Finally, taking the scalar and vector products of equation (2*b*) with $\boldsymbol{h}$, we get the radial and poloidal equilibrium conditions, which are valid for low-β plasmas:

$$J_\theta B \approx \nabla_r p_{\rm eq}, \qquad \rho_1 = \gamma(2M_{\rm p}^2 - 2M_{\rm p}M_{\rm t} + M_{\rm t}^2)(1-\gamma M_{\rm p}^2)^{-1} \tag{3}$$

where $M_{\rm p}^2 = u_0^2/(c_{\rm s}^2 h_\theta^2)$, $M_{\rm t}^2 = U^2/c_{\rm s}^2 \ll 1$ are the poloidal and toroidal Mach numbers and $c_{\rm s}^2 = \gamma P/\rho$. We note that the equation for ρ_1 is the same as that used in [10] in addition to the γ-coefficient that appears due to our isothermal equilibrium in place of the adiabatic one. On the other hand, the radial ion temperature gradient (or drift velocity) establishes the next relation with the poloidal flow due to the simplest model of the heat balance equation (1):

$$u_* = \frac{\nabla v_{\rm Ti}^2}{\omega_{\rm ci0}} = \left(1-\frac{1}{\gamma}\right)\left(1+\frac{T_{\rm e}}{T_{\rm i}}\right)u_0 M_{\rm p}^2. \tag{4}$$

3. Evaluation of dispersion relations

To begin the perturbative analysis, we expand the set of oscillating amplitudes $\{p, v_{||}, \tilde{\rho}\}$ in Fourier series over the poloidal angle, as for density $\tilde{\rho} = \rho_0(\tilde{\rho}_0 + \rho_c\cos\theta + \rho_s\sin\theta)$, where the first harmonic is only taken into account and the effect of second harmonics is considered as the second ε-order corrections to the main terms. In this case, perturbations with a constant amplitude over angle are also ignored (for example, $\tilde{\rho}_0 = \varepsilon\cdot\rho_c/2$ that comes directly from equation (2*a*)). We change the radial electric field for v_b-variable, $v_b = -c\tilde{E}_r/B_0$, which is independent of θ. Next, substituting the perturbed values into equation (1), (2*a*)–(2*c*) and using the vector and scalar products of equation (2*b*) with the $\boldsymbol{h}$-vector, we obtain the equations for pressure, density and parallel velocity oscillations:

$$p_{\rm s} = \gamma\rho_{\rm s} + \mathrm{i}M_{\rm p}p_c/\Omega - \mathrm{i}\,(\gamma-1)\,q\rho_1 h_\zeta v_b/\Omega c_{\rm s} - \mathrm{i}\gamma\,(1-M_d)\,M_{\rm p}\rho_c/\Omega \tag{5a}$$

$$p_c = \gamma\rho_c - \mathrm{i}M_\mathrm{p}p_\mathrm{s}/\Omega + \mathrm{i}\gamma\,(1 - M_d)\,M_\mathrm{p}\rho_\mathrm{s}/\Omega \tag{5b}$$

$$\mathrm{i}\Omega c_\mathrm{s}\rho_c = v_\mathrm{s} + c_\mathrm{s}M_\mathrm{p}\rho_\mathrm{s} \tag{5c}$$

$$\mathrm{i}\Omega c_\mathrm{s}\rho_\mathrm{s} = -2q_M v_b - v_c - c_\mathrm{s}M_\mathrm{p}\rho_c \tag{5d}$$

$$\mathrm{i}\Omega v_\mathrm{s} = (2q_M M_\mathrm{p} - q\,M_\mathrm{t})v_b - M_\mathrm{p}v_c - c_\mathrm{s}p_c/\gamma \tag{5e}$$

$$\mathrm{i}\Omega v_c = M_\mathrm{p}v_\mathrm{s} + c_\mathrm{s}p_\mathrm{s}/\gamma \tag{5f}$$

where $q_M = q[1 + \gamma(M_\mathrm{t}^2/2 - M_\mathrm{p}M_\mathrm{t})](1 - \gamma M_\mathrm{p}^2)^{-1}$, $\Omega = \omega R_0 q/c_\mathrm{s}$, is the normalized frequency, $M_d = (1 - 1/\gamma)\rho_1(2 + \rho_1)^{-1}$ is the parameter responsible for the heat flux effect and the approximation $|h_\zeta| \approx 1$ is used. Then, to get the geodesic continuum frequency we employ the current continuity equation for the perturbed current $\nabla \cdot \boldsymbol{j}_\perp = 0$, where only $\cos\theta$-pressure perturbations contribute because of the standard averaging procedure over the magnetic surfaces used to evaluate geodesic modes:

$$\oint R(\nabla \cdot \boldsymbol{j}_\perp)\,\mathrm{d}\theta = R_0\nabla_r\langle j\rangle = \frac{\mathrm{i}\Omega c_\mathrm{s}c\rho_0}{B_0 q}\frac{\mathrm{d}}{\mathrm{d}r}\left[v_b + \mathrm{i}q\frac{c_\mathrm{s}p_\mathrm{s}}{\gamma\Omega} + \mathrm{i}q\frac{c_\mathrm{s}\rho_\mathrm{s}}{2\Omega}M_\mathrm{t}^2 + \mathrm{i}\frac{q\,v_\mathrm{s}}{\Omega}M_\mathrm{t}\right] = 0 \tag{6}$$

where the averaged current may be presented via the dielectric tensor $\langle j_r\rangle = (-\mathrm{i}\omega/4\pi)\varepsilon_0 E_r$.

Finally, using combinations of equation (5*a*)–(5*f*), we calculate the perturbed pressure, density and velocity, which are introduced into equation (6) to obtain the geodesic continuum equation through the radial tensor component:

$$\varepsilon_0 = \frac{c^2}{c_\mathrm{A}^2}\frac{(\Omega^2 - \Omega_1^2)(\Omega^2 - \Omega_2^2)(\Omega^2 - \Omega_3^2) + \delta N}{[\Omega^4 - 2\Omega^2(1 + M_\mathrm{p}^2 + M_\mathrm{p}^2M_d) + 1 - 2M_\mathrm{p}^2(M_\mathrm{p}^2 - M_d)^2](\Omega^2 - \Omega_{d3}^2) + \delta D} = 0 \tag{7}$$

where c_A is the Alfvén velocity. Exact expressions in the numerator of the above equation are very long and we present them in an approximated form, which are shown in the appendix. The corrections δN, $\delta D \approx O(\rho_1^3)$ have the order of ρ_1^3, which will be ignored in our study. In the denominator, we find the roots $\Omega_{d1,2}^2 = (1 \pm M_\mathrm{p})^2 \pm (1 \mp M_\mathrm{p})M_\mathrm{p}M_d + O(\rho_1^3)$, and $\Omega_{d3}^2 = M_\mathrm{p}^2(1 - M_d)^2 + O(\rho_1^3)$. Two roots $\Omega_{1,2}^2$ of the numerator correspond to the $\mathrm{GAM}_{1,2}$ branches. Keeping terms of the order of ρ_1 or terms M_p^2, $M_\mathrm{p}M_\mathrm{t}$, M_t^2, we get from equation (A3)

$$\omega_\mathrm{GAM1}^2 = \left[2 + \frac{1}{q^2} + \left(2 - \frac{1}{q^2} + \frac{2}{q^4}\right)M_\mathrm{p}^2 + 4M_\mathrm{t}^2 - 4\left(1 - \frac{1}{q^2}\right)M_\mathrm{p}M_\mathrm{t}\right]c_\mathrm{s}^2/R_0^2 \tag{8a}$$

$$\omega_\mathrm{GAM2}^2 = \left[1 + \left(3 - \frac{2}{q^2}\right)M_\mathrm{p}^2 - 4M_\mathrm{p}M_\mathrm{t}\right]c_\mathrm{s}^2/q^2R_0^2 \tag{8b}$$

which are slightly modified by the poloidal rotation with corrections of the order of ρ_1^2. These geodesic modes have also been discussed in [10]. First GAM branch (8*a*) exactly coincides with the one presented in [7] for $M_\mathrm{p} = 0$ and it is similar to [9] in the limit $M_\mathrm{t} = 0$. We note that the sound branch $\Omega_2^2 \approx 1 + (3 - 2/q^2)M_\mathrm{p}^2 - 4M_\mathrm{p}M_\mathrm{t}$ stays in the frequency band between the denominator roots $\Omega_{d12}^2 \approx 1 \pm 2\sqrt{M_\mathrm{p}^2}$ in equation (7). This means that the branch is degenerated in the limit $M_\mathrm{p} = 0$ due to the factors $(\Omega \pm 1)$, which are divided out in the fraction (7). Most interesting is the third new root in the numerator of equation (7), which depends only on the poloidal/toroidal circulation frequency,

$$\omega_\mathrm{ZF}^2 = \left[M_\mathrm{p}^2(1 - M_d)^2 + \frac{q^2(\gamma - 1)}{2(1 + 2q^2)}(M_\mathrm{t}^2 - 2M_\mathrm{t}M_\mathrm{p} + 2M_\mathrm{p}^2)M_\mathrm{t}^2\right]\frac{c_\mathrm{s}^2}{q^2R_0^2}. \tag{9}$$

The frequency of this branch is small in comparison with the geodesic ones in equations (8*a*) and (8*b*).

4. Discussion and summary

The ZF mode (9) may be referred to as the geodesic Doppler mode in the case of preferentially poloidal rotation, which appears due to the isothermal pressure profile. This branch has a frequency higher than the lower denominator root, $\omega_{d3}^2 = (1 - M_d)^2(M_\mathrm{p}^2 c_\mathrm{s}^2/q^2 R_0^2)$. This means that the ZF branch may disappear in the formal limit $M_\mathrm{t}^2 = 0$ when the factors $[\Omega^2 - M_\mathrm{p}^2(1 - M_d)^2]$ are divided out in the fraction in equation (7). The mode frequency stays at the poloidal circulation frequency u_0/r when toroidal rotation is not yet too small, $M_\mathrm{t}^4 \ll M_\mathrm{p}^2 \sim M_\mathrm{t}^2$. In the case of preferentially toroidal rotation $M_\mathrm{t}^4 \gg M_\mathrm{p}^2$ in equation (9), we have the result of [7].

We note that real eigenmodes may only propagate at the maximum or minimum of the continuum [11]. In the opposite case, they convert themselves at the continuum frequency into short radial wave oscillations, which usually have strong dissipation. It is very important to take into account the Alfvén wave continuum (AWC) to verify transitions of the continuum branches and to know where continuum extremum may occur. In a quasi-cylindrical approach [11], the AWC equation may be written in the form

$$\varepsilon_0 \frac{\omega^2 R^2}{c^2 R_0^2} E_r = \hat{k}_{||}^2 E_r = \frac{1}{q^2 R^2} \left(nq - \frac{\mathrm{d}}{\mathrm{d}\theta} \right)^2 E_r. \tag{10}$$

Therefore, there is bifurcation of the continuum modes at the rational magnetic surfaces. To show transitions between the continuum branches, the squared frequency of the continuum is plotted schematically as a function of q at the rational surface defined by $m = 3$, $n = 2$ poloidal/toroidal mode numbers in figure 1. Typical tokamak plasma parameters $r = 0.1R_0$, $(c_\mathrm{A}/c_\mathrm{s}) = 10$ and $c/c_\mathrm{A} = 100$ are chosen for preferentially poloidal ($M_\mathrm{p} = 0.5$, $M_\mathrm{t} = 0.05$) and toroidal ($M_\mathrm{p} = 0.05$, $M_\mathrm{t} = 0.5$) rotation. The Mach numbers are taken large enough for better visualization of the curves in the figure. In figure 1, we can observe that the AWC appears above the standard GAM_1, ion-sound continuum may occupy the narrow band limited by the poloidal Mach number, $1 - 2\sqrt{M_\mathrm{p}^2} < \omega^2/\omega_{\mathrm{GAM2}}^2 < 1 + 2\sqrt{M_\mathrm{p}^2}$. Moreover, we have the ZF continuum that superposes the frequency band from the ZF frequency up to the sound frequency band, $(\gamma - 1)V^4/(2 + 4q^2) < \omega^2 c_\mathrm{s}^2 R_0^2 < (1 - 2\sqrt{M_\mathrm{p}^2})c_\mathrm{s}^4/q^2$.

Finally, we conclude that the complete plasma equilibrium with rotation is very important for analyses of the ZF and geodesic continuum modes. We find that there are three branches of the geodesic continuum in rotating plasmas with isothermal magnetic surfaces, which are the standard GAM, the ion-sound and ZF modes. In the case of the adiabatic equilibrium, there are only two geodesic continuum branches that are the standard GAM and the ion-sound modes. In the case of the isothermal surfaces with poloidal rotation, the heat flow should be taken into account. It produces a small modification in the standard $\mathrm{GAM}_{1,2}$ modes but it also modifies the ZF mode, which appears as some Doppler mode for preferentially poloidal rotation. Intersection of the AWC at the rational magnetic surface with the geodesic ones produces continuum gaps where some eigenmodes may propagate. The standard Alfvén continuum appears above the standard GAM_1 and the sound continuum ω_{GAM2} may occupy the narrow band at the ion-sound frequency limited in the band, whose width is defined by the frequency of the order of the poloidal rotation frequency. The combined ZF + AW continuum superposes the frequency band from the effective 'gravity' mode up to the ion-sound one, which may be very important to suppress the turbulence in this frequency band.

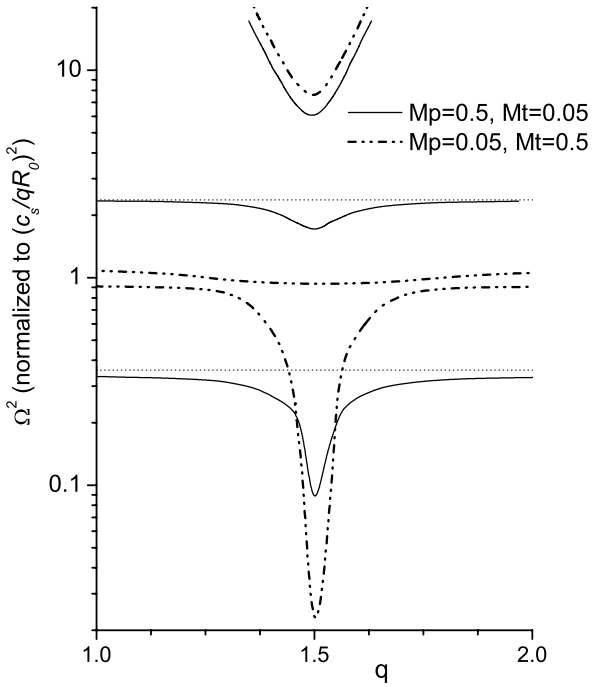

Figure 1. Schematic plot of bifurcation of Alfvén continuum by the geodesic one for preferentially poloidal rotation with $M_\mathrm{p} = 0.5$, $M_\mathrm{t} = 0.05$ (solid lines), and for preferentially toroidal rotation with $M_\mathrm{p} = 0.05$, $M_\mathrm{t} = 0.5$ (dashed–dotted–dotted lines); additional dotted lines show the ion-sound limits $\Omega^2_{d12} = 1 \pm 2\sqrt{M^2_\mathrm{p}}$ of the Alfvén geodesic continuum for $M_\mathrm{p} = 0.5$, $M_\mathrm{t} = 0.05$.

Appendix

The dispersion equation at the numerator in equation (7) is presented in the form

$$\Omega^6 - \Omega^4[2 + 2q^2(1 + 2M_\mathrm{t}^2 + M_\mathrm{p}^2 - 2M_\mathrm{p}M_\mathrm{t}) + 3M_\mathrm{p}^2] + \Omega^2[1 + 2q^2(1 + 2M_\mathrm{t}^2 + 5M_\mathrm{p}^2 - 6M_\mathrm{p}M_\mathrm{t})] - M_\mathrm{p}^2(1 + 2q^2) + P_4 = 0 \qquad \text{(A1)}$$

where polynomial P_4 contains the corrections of the order of $O(\rho_\mathrm{i}^2)$ due to rotation:

$$\begin{aligned} P_4 = {} & q^2\gamma(2M_\mathrm{t}^3M_\mathrm{p} + 4M_\mathrm{p}^3M_\mathrm{t} - 2M_\mathrm{p}^4 - 4M_\mathrm{t}^2M_\mathrm{p}^2 - M_\mathrm{t}^4/2)\Omega^4 + \{3M_\mathrm{p}^2(M_\mathrm{p}^2 - 2M_d) \\ & + q^2[(4 + 6\gamma)M_\mathrm{p}^4 - 3(\gamma + 1)M_\mathrm{t}^3M_\mathrm{p} - 2M_d(M_\mathrm{p}^2 + 2M_\mathrm{t}M_\mathrm{p}) + (7\gamma + 13)M_\mathrm{t}^2M_\mathrm{p}^2 \\ & + (\gamma - 1/2)M_\mathrm{t}^4 - (8\gamma + 12)M_\mathrm{p}^3M_\mathrm{t}]\}\Omega^2 + 2(M_d + M_\mathrm{p}^2)M_\mathrm{p}^2 \\ & - q^2[8M_\mathrm{p}^4 + (3 + \gamma)M_\mathrm{t}^2M_\mathrm{p}^2 + (\gamma - 1)(M_\mathrm{t}/2 - M_\mathrm{p})M_\mathrm{t}^3 - 12M_\mathrm{p}^3M_\mathrm{t} - 4M_dM_\mathrm{p}^2]. \end{aligned} \qquad \text{(A2)}$$

We find that equation (A1) has the same factor $f_\mathrm{ct} = (\Omega^2 - M_\mathrm{p}^2(1 - M_d)^2)$ as the denominator in equation (7) in the formal limit $M_\mathrm{t}^2 = 0$. This means that some new root may appear at the frequency $\Omega^2_{3d} = M_\mathrm{p}^2(1 - M_d)^2$ in the case of $M_\mathrm{t}^2 \neq 0$. The velocity corrections to standard GAMs can be found from equation (A1), which is divided by f_st-factor. As a result, we get the equation

$$\Omega^4 - 2\Omega^2[1 + M_\mathrm{p}^2 + q^2(1 + 2M_\mathrm{t}^2 + M_\mathrm{p}^2 - 2M_\mathrm{p}M_\mathrm{t})] + 2q^2(1 + 2M_\mathrm{t}^2 + 4M_\mathrm{p}^2 - 6M_\mathrm{p}M_\mathrm{t}) + 1 - 2M_\mathrm{p}^2 + S_4 = R_4/f_\mathrm{st} \qquad \text{(A3)}$$

where

$$S_4 = \Omega^2[q^2\gamma(4M_p^3M_t + 2M_t^3M_p - 2M_p^4 - 4M_p^2M_t^2 - M_t^4/2) - 2M_p^2M_d] + M_p^4 - 2M_p^2M_d + q^2\{(6\gamma+2)M_p^4 + [(7\gamma+9)M_t^2 + 2M_d]M_p^2 - [8(\gamma+1)M_p^2 + 3(\gamma+1)M_t^2 + 4M_d]M_tM_p + (\gamma - 1/2)M_t^4\}$$

and the rest of the division $R_4 = (\gamma-1)q^2(M_t^2/2 - M_tM_p + M_p^2)M_t^2$ are shown with accuracy $O(\rho_1^2)$. In the first-order approach $O(\rho_1)$, the equation for $\Omega_{1,2}^2$ has the form

$$\Omega_{(0)1,2}^2 \approx 1 + M_p^2 + q^2(1 - 2M_pM_t + M_p^2 + 2M_t^2) \pm \sqrt{q^4(1 - 4M_pM_t + 2M_p^2 + 4M_t^2) + 4q^2(2M_pM_t - M_p^2) + 4M_p^2} \tag{A4}$$

which are shown in equations (8*a*) and (8*b*). Further, $\Delta_{1,2}$-corrections of the order $O(\rho_1^2)$ to the $\Omega_{(0)1,2}^2$ roots can be easily calculated from equation (A3):

$$\Delta_{1,2} = (R_4/\Omega_{(0)1,2}^2 - S_4)/(2\Omega_{(0)1,2}^2 - 2).$$

Finally, taking into account the next order terms $O(\rho_1^2)$ in equation (A3) together with the rest of the division R_4, we calculate the third root, $\Omega_3^2 = \Omega_{3d}^2 + R_4/\Omega_1^2\Omega_2^2 \approx M_p^2(1 - M_d)^2 + R_4/(2q^2+1)$, which is shown in equation (9).

Acknowledgments

The authors are grateful to the CNPq (National Council of Brazil for Science and Technology Development) and to the FINEP (Financiadora de Estudos e Projetos) for financial support.

References

[1] Winsor N, Jonson J L and Dowson J M 1968 *Phys. Fluids* **11** 2448
[2] Krämer-Flecken A, Soldatov S, Koslowski H R and Zimmermann O 2006 *Phys. Rev. Lett.* **97** 045006
[3] McKee G R *et al* 2009 *Nucl. Fusion* **49** 115016
[4] Conway G D *et al* 2005 *Plasma Phys. Control. Fusion* **47** 1165–85
[5] Conway G D *et al* 2011 *Phys. Rev. Lett.* **106** 065001
[6] van der Holst B, Beliën A J C and Goedbloed J P 2000 *Phys. Plasmas* **7** 4208
[7] Wahlberg C 2008 *Phys. Rev. Lett.* **101** 115003
[8] Lakhin V P, Ilgisonis V I and Smolyakov A I 2010 *Phys. Lett.* A **374** 4872
[9] Zhou D 2010 *Phys. Plasmas* **17** 102505
[10] Ilgisonis V I, Lakhin V P, Sorokina E A and Smolyakov A I 2010 *Proc. 23rd Int. Conf. on Fusion Energy 2010 (Daejeon, Korea)* (Vienna: IAEA) THS/P8-01
[11] Elfimov A G 2010 *Phys. Plasmas* **17** 022102
[12] Zonca F and Chen L 2008 *Europhys. Lett.* **83** 35001
[13] Braginskii S I 1965 *Review of Plasma Physics* vol 1, ed M A Leontovch (New York: Consultants Bureau) p 205